

H₂O₂-Independent Chemodynamic Therapy Initiated from Magnetic Iron Carbide Nanoparticle-Assisted Artemisinin Synergy

Fan Zhao,^{†ab} Jing Yu,^{†ab} Weiliang Gao,^{ab} Xue Yang,^c Liying Liang,^{ab} Xiaolian Sun,^d Dan Su,^e Yao Ying,^{ab} Wangchang Li,^{ab} Juan Li,^{ab} Jingwu Zheng,^{ab} Liang Qiao,^{ab} Wei Cai,^{ab} Shenglei Che,^{*ab} and Xiaozhou Mou^{*c}*

a. College of Materials Science and Engineering, Zhejiang University of Technology, Hangzhou 310014, China. E-mail: yujing@zjut.edu.cn; cheshenglei@zjut.edu.cn.

b. Research Center of Magnetic and Electronic Materials, Zhejiang University of Technology, Hangzhou 310014, China.

c. Clinical Research Institute, Zhejiang Provincial People's Hospital, Hangzhou 310014, China. E-mail: mouxz@zju.edu.cn.

d. Key Laboratory of Drug Quality Control and Pharmacovigilance (China Pharmaceutical University), Ministry of Education, Nanjing 210009, China.

e. Department of Oncology, Zhejiang Provincial People's Hospital, Hangzhou 310014, China

† These authors contributed equally to this manuscript.

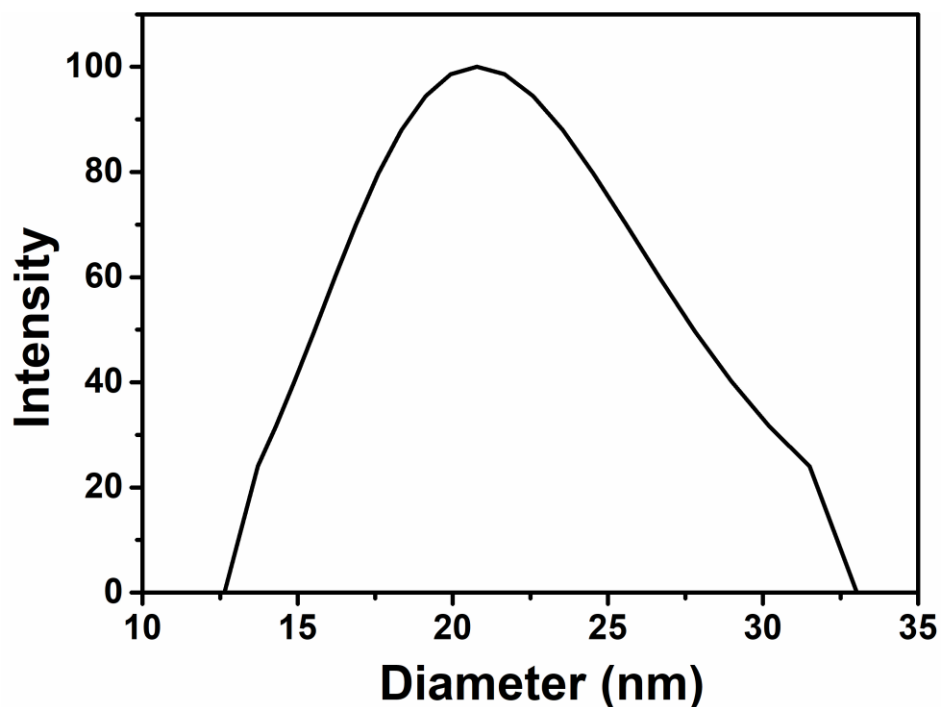


Figure S1. DLS spectrum of $\text{Fe}_2\text{C}@\text{Fe}_3\text{O}_4$ NPs.

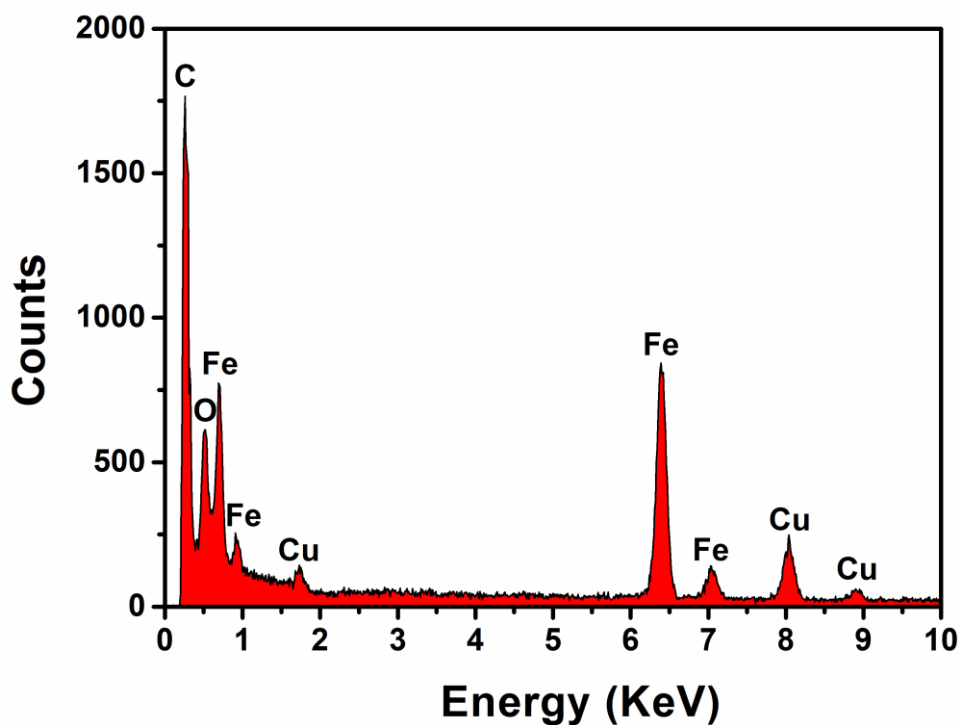


Figure S2. The energy spectrum of $\text{Fe}_2\text{C}@\text{Fe}_3\text{O}_4$ NPs.

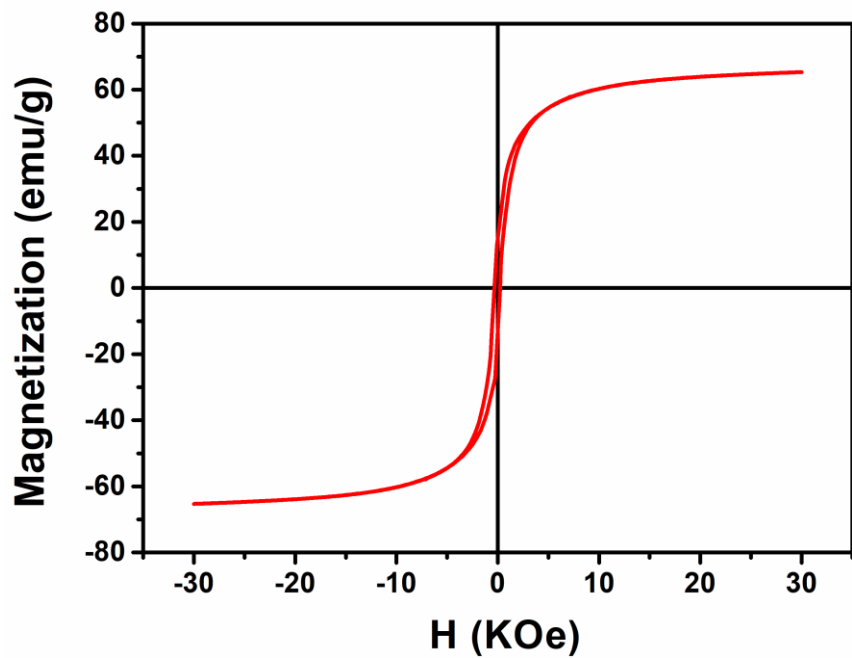


Figure S3. Room-temperature magnetic hysteresis loops of $\text{Fe}_2\text{C}@\text{Fe}_3\text{O}_4$ NPs.

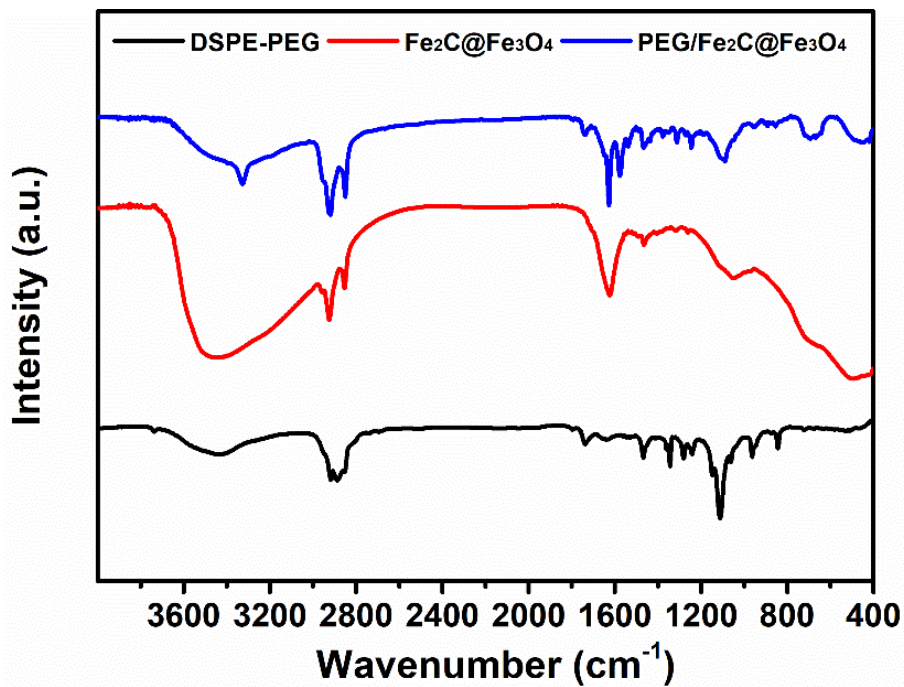


Figure S4. FT-IR spectra of DSPE-PEG, $\text{Fe}_2\text{C}@\text{Fe}_3\text{O}_4$, and $\text{PEG}/\text{Fe}_2\text{C}@\text{Fe}_3\text{O}_4$ NPs.

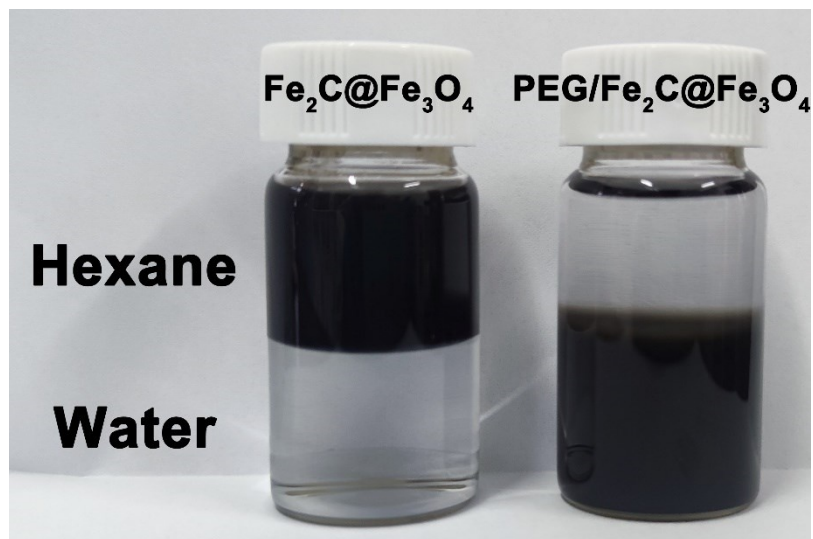


Figure S5. Digital graph of Fe₂C@Fe₃O₄ and PEG/Fe₂C@Fe₃O₄ NPs dispersed in hexane or water.

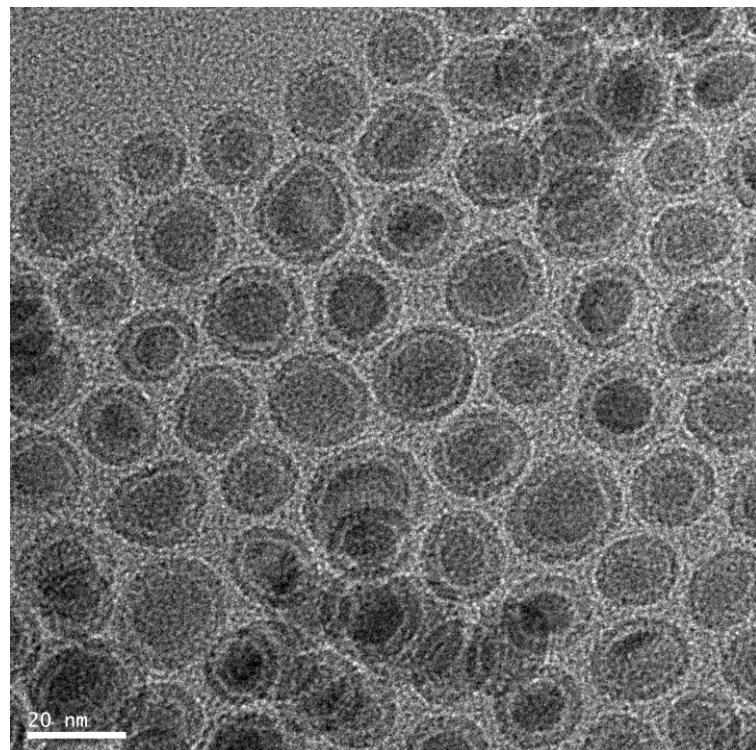


Figure S6. TEM image of PEG/Fe₂C@Fe₃O₄.

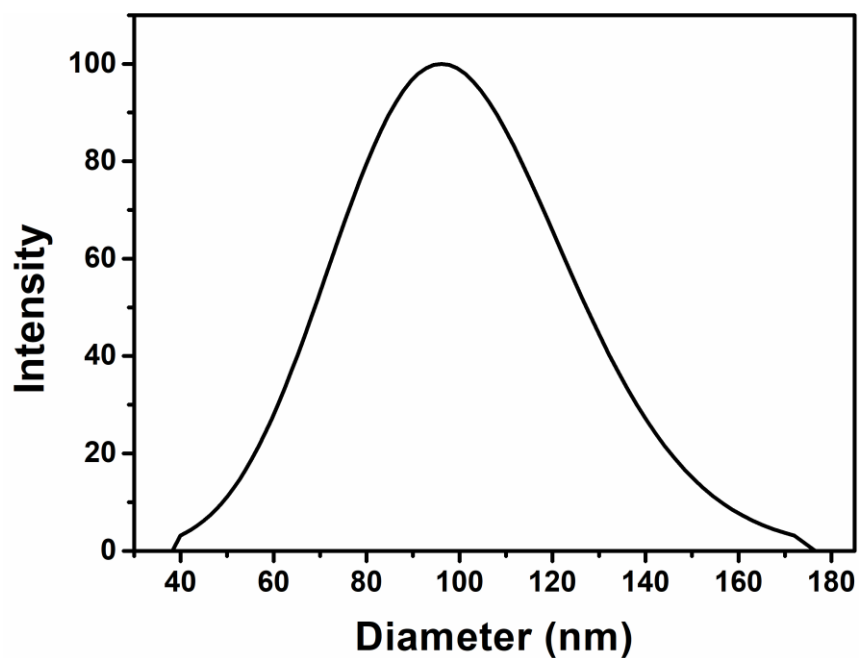


Figure S7. DLS spectrum of PEG/Fe₂C@Fe₃O₄ NPs.

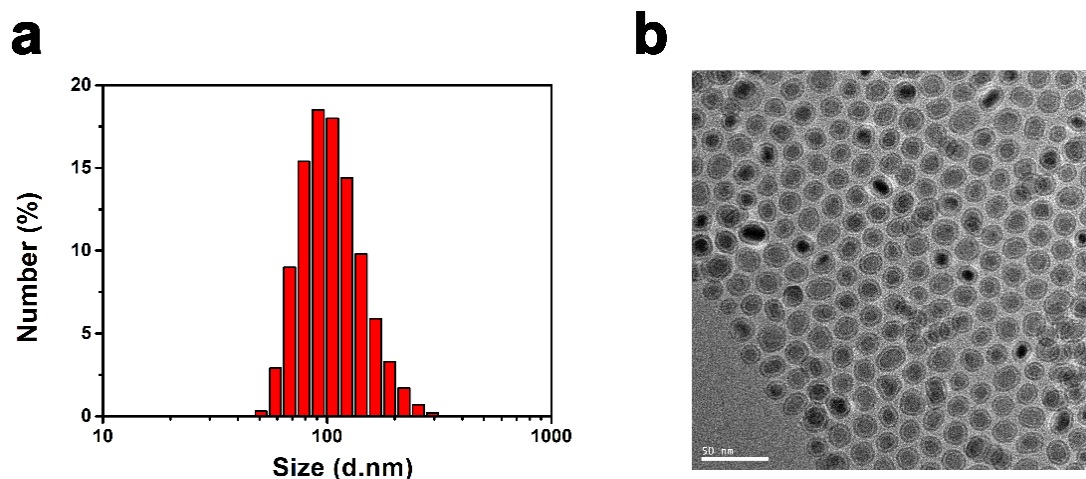


Figure S8. (a) DLS spectrum of PEG/Fe₂C@Fe₃O₄ NPs after 7 days storage. (b) TEM image of PEG/FeC₂@Fe₃O₄ NPs after 7 days storage.

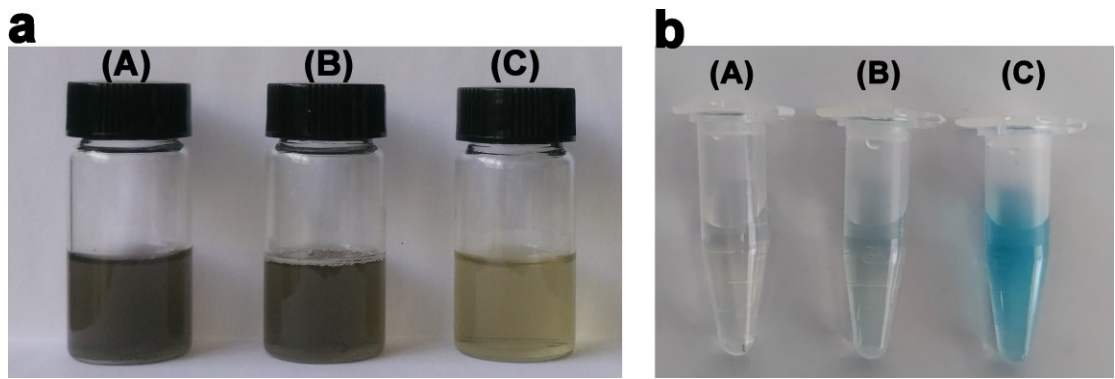


Figure S9. (a) Photo of PEG/Fe₂C@Fe₃O₄ NPs dispersing in (A) pH 7.4, (B) pH 6.5 and (C) pH 5.4 for 24 h. (b) Photo of potassium ferricyanide (Fe²⁺ indicator) dispersed in the supernatant of PEG/Fe₂C@Fe₃O₄ NPs in (A) pH 7.4, (B) pH 6.5 and (C) pH 5.4.

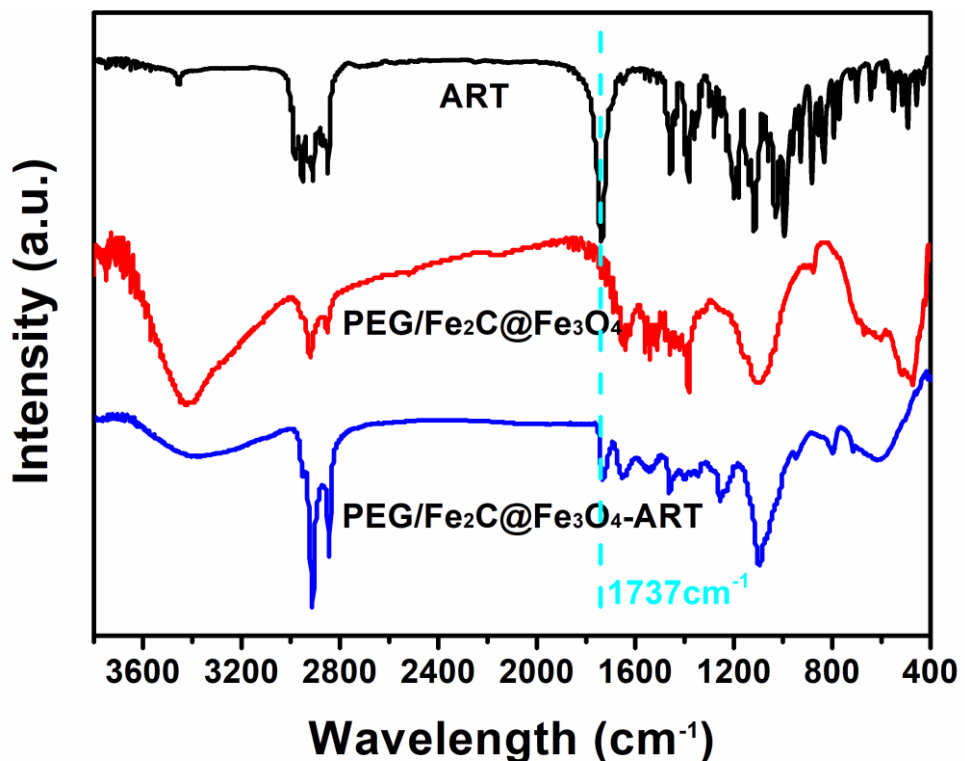


Figure S10. FT-IR spectra of standard ART, PEG/Fe₂C@Fe₃O₄ NPs and ART-loaded PEG/Fe₂C@Fe₃O₄ NPs.

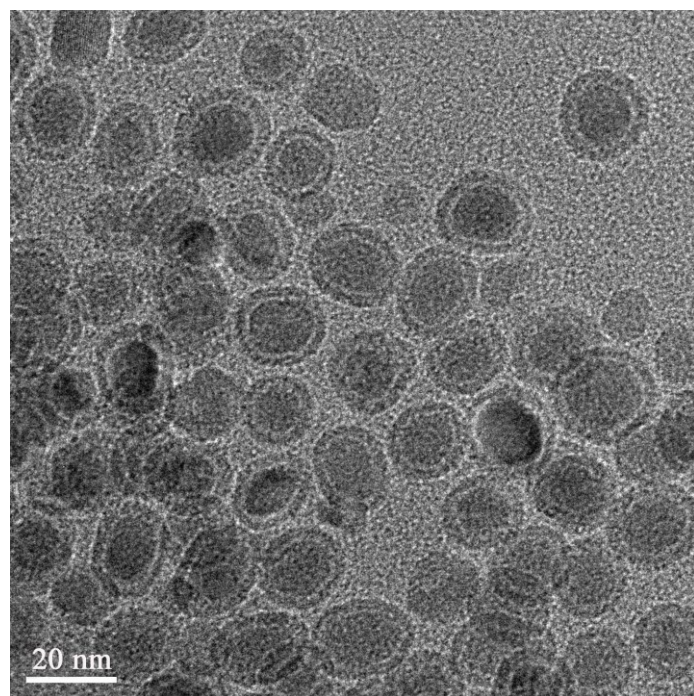


Figure S11. TEM image of PEG/Fe₂C@Fe₃O₄-ART.

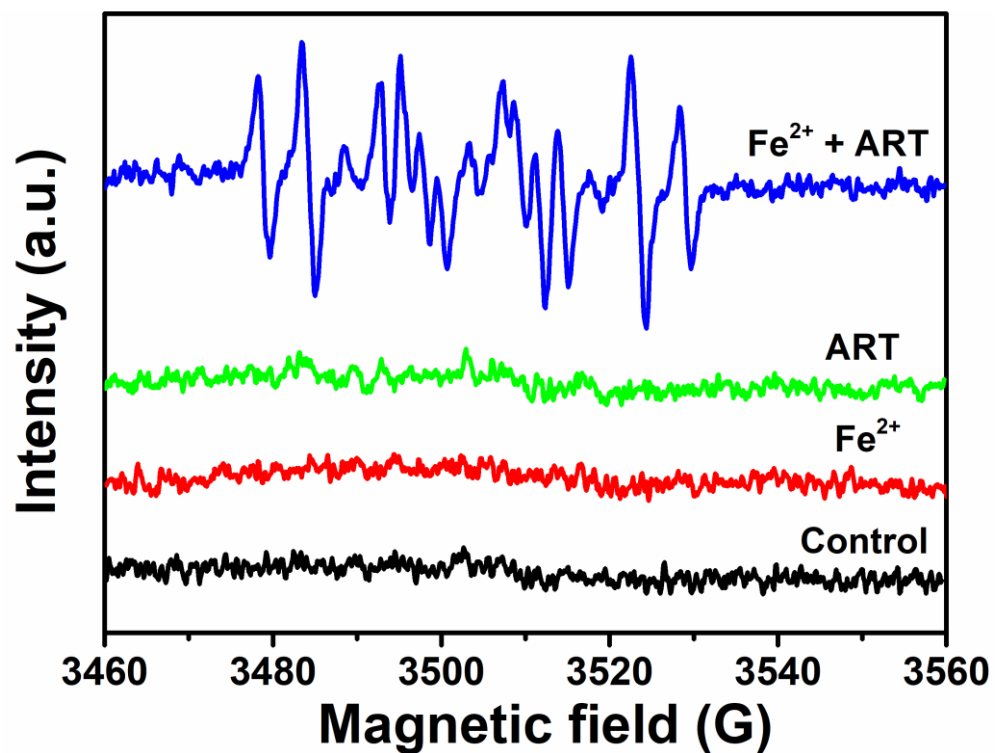


Figure S12. ESR measurements of free radical formation by ART with Fe²⁺.

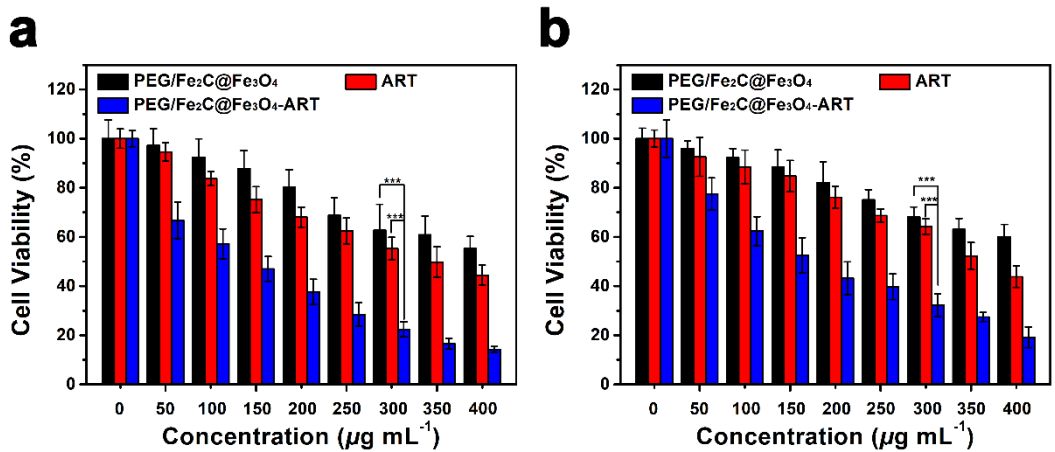


Figure S13. Viability of HeLa (a) and MDA-MB-231 (b) cells after different treatments under various conditions for 24 h ($n = 6$, mean \pm s.d., *** $p < 0.001$).

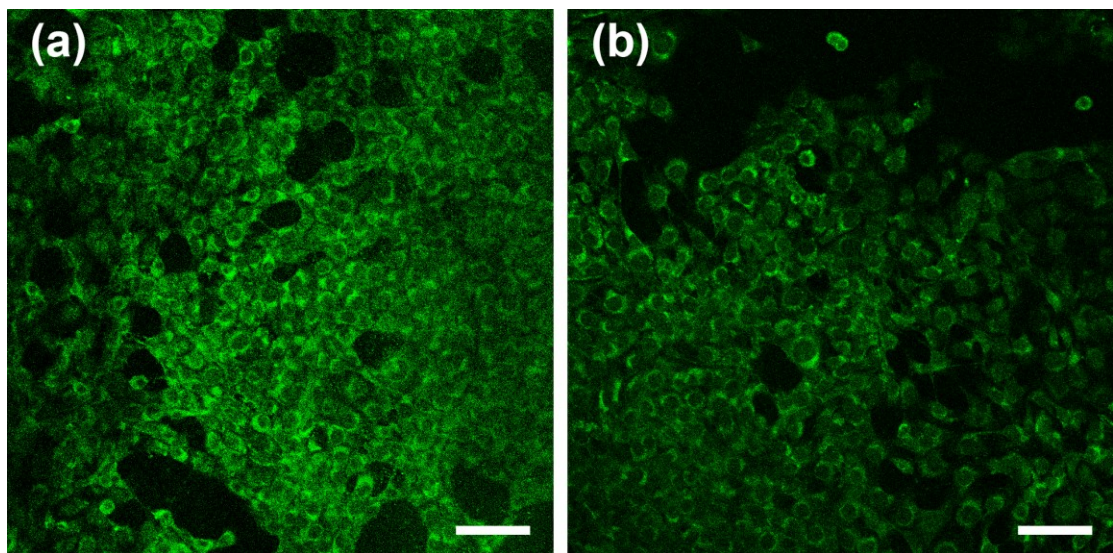


Figure S14. Fluorescence images of DCFH-DA labeled 4T1 cells treated by (a) PEG/Fe₂C@Fe₃O₄-ART and (b) PEG/Fe₂C@Fe₃O₄-ART plus 2,2-bipyridyl under magnetic targeting. Scale bars are 75 μm .

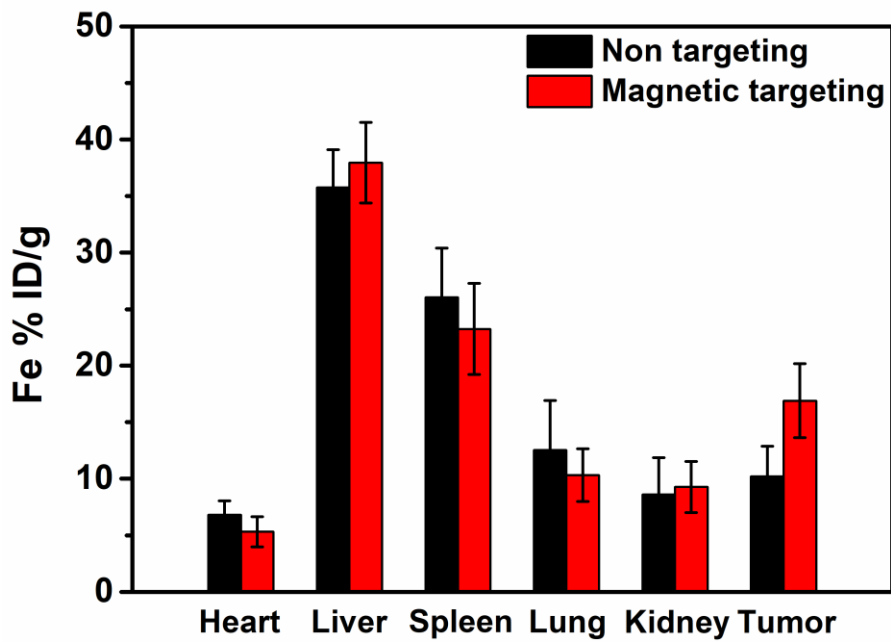


Figure S15. The biodistribution of Fe (% administrated dose (ID) of Fe per gram of tissues) in main tissues and tumors after intravenous administrations with or without magnetic targeting for 24 h.

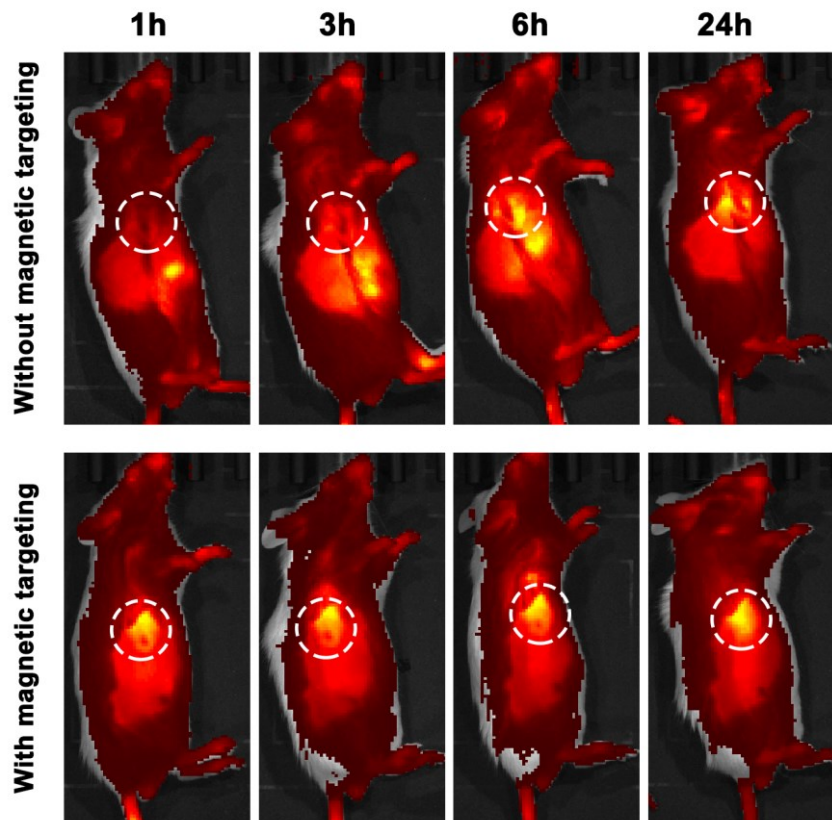


Figure S16. In vivo NIR imaging of tumor-bearing mice after intravenous injection of IR783-labeled $\text{Fe}_2\text{C}@\text{Fe}_3\text{O}_4$ NPs at 1, 3, 6, and 24 h post-injection (White circled area: tumor site).

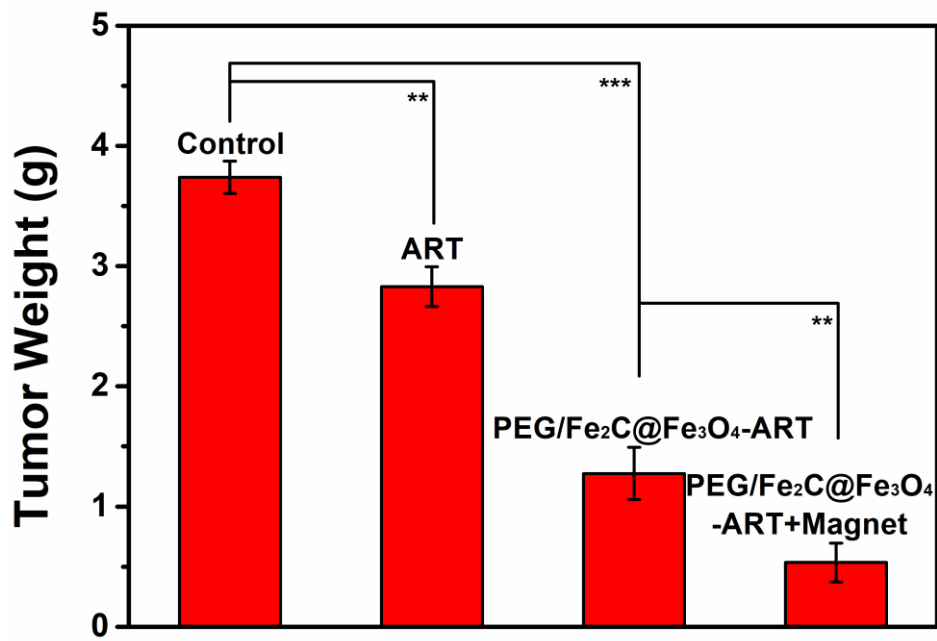


Figure S17. Average tumor mass excised from the 4T1 tumor-bearing mice after treatment ($n = 5$, mean \pm s.d., ** $p < 0.01$, *** $p < 0.001$).

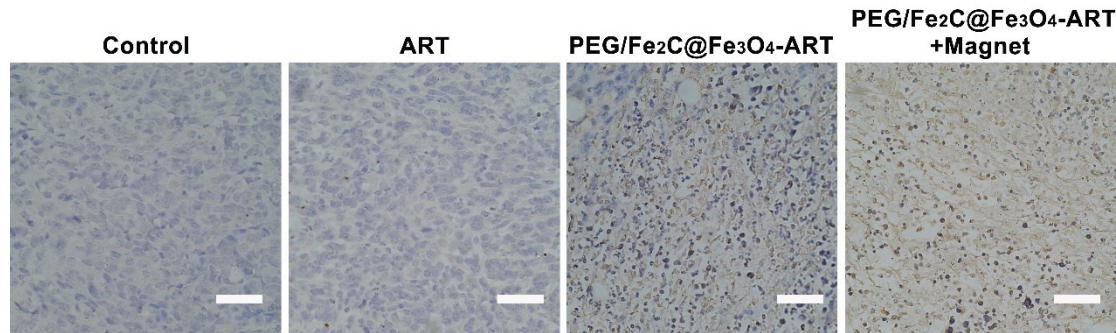


Figure S18. TUNEL staining of 4T1 tumor sections in different groups. (scale bar 100 μ m)

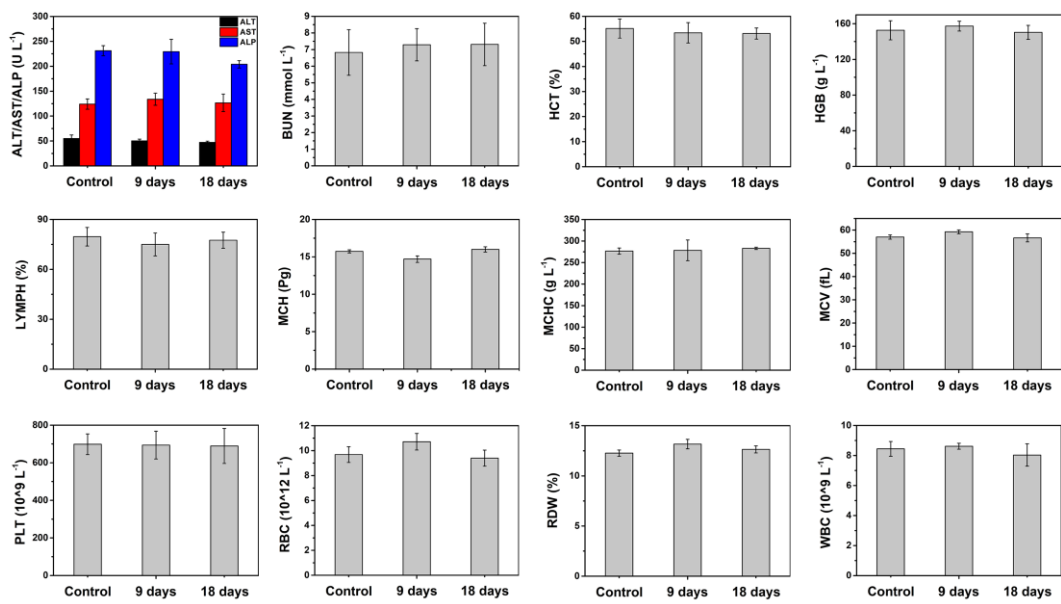


Figure S19. Blood panel analysis and blood biochemistry test of healthy mice after intravenous injection of PEG/Fe₂C@Fe₃O₄-ART NPs with different time (9 days or 18 days).

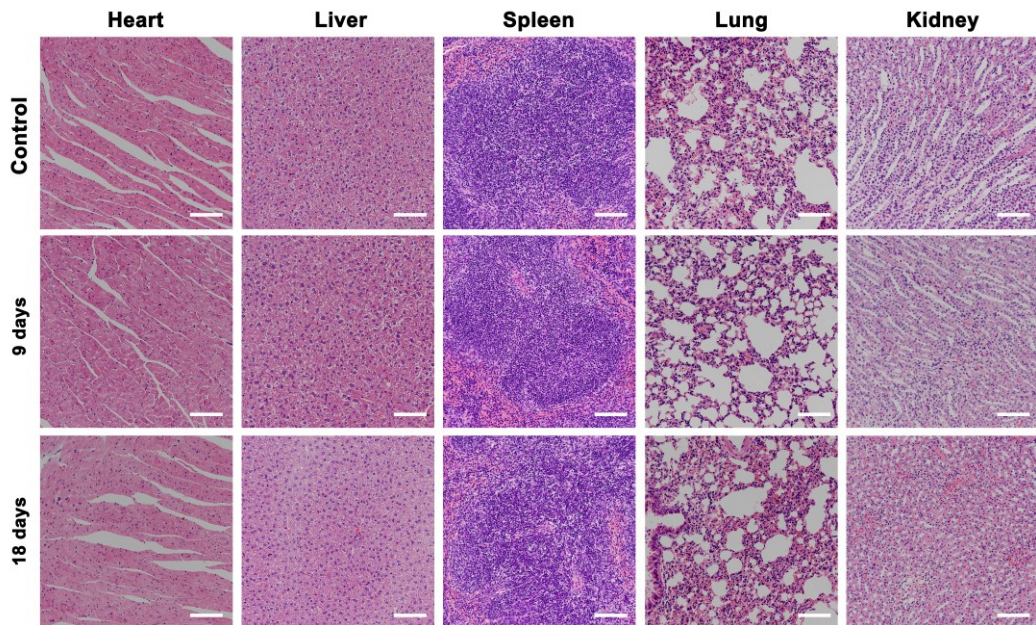


Figure S20. H&E staining images of major organs (heart, liver, spleen, lung, kidney) of the mice after injection of PEG/Fe₂C@Fe₃O₄-ART NPs with different time (9 days or 18 days) (scale bar 100 μ m).